THESIS FOR THE DEGREE OF DOCTOR OF PHILOSOPHY

Moisture and Chloride Transport in Concrete

Mesoscale Modelling and Computational Homogenization

FILIP NILENIUS

Department of Civil and Environmental Engineering
Division of Structural Engineering, Concrete Structures
CHALMERS UNIVERSITY OF TECHNOLOGY

Gothenburg, Sweden 2014

Moisture and Chloride Transport in Concrete
Mesoscale Modelling and Computational Homogenization
FILIP NILENIUS
ISBN 978-91-7385-977-6

© FILIP NILENIUS, 2014

Doktorsavhandlingar vid Chalmers tekniska högskola
Ny serie nr. 3658
ISSN 0346-718X
Department of Civil and Environmental Engineering
Division of Structural Engineering, Concrete Structures
Chalmers University of Technology
SE-412 96 Gothenburg
Sweden
Telephone: +46 (0)31-772 1000

Colophon:
The thesis was created using LaTeX 2$_\varepsilon$ and edited in Texmaker. The typesetting software was the TeX Live distribution. The text is set in Palatino, the plots were constructed by PGF/Ti*k*Z and the figures were constructed by PGF/Ti*k*Z, Incscape and ParaView.

Cover:
Photo showing the strongly heterogeneous mesoscale structure of concrete.

Chalmers Reproservice
Gothenburg, Sweden 2014

Moisture and Chloride Transport in Concrete
Mesoscale Modelling and Computational Homogenization
Thesis for the degree of Doctor of Philosophy
FILIP NILENIUS
Department of Civil and Environmental Engineering
Division of Structural Engineering, Concrete Structures
Chalmers University of Technology

Abstract

Material properties pertaining to the physical phenomena of mass transport in concrete are important for the durability of concrete structures, and they can ultimately be derived from material heterogeneities found at different subscales. On the mesoscale level, these heterogeneities are mainly characterized by the presence of embedded aggregates in the cement paste, together with cracks.

This thesis concerns modelling of moisture and chloride transport in concrete, where the mesoscale heterogeneities are explicitly accounted for by means of geometrical and constitutive descriptions along with computational homogenization. The objective of this work was to numerically study how the heterogeneous and random mesoscale composition of concrete influence the homogeneous transport properties on the macroscale. This objective was ultimately met by the development of two- and three-dimensional Statistical Volume Elements (SVEs) of mesoscale concrete, which are geometrical representations of the material morphology. The developed SVEs contained the mesoscale constituents cement paste, aggregates and the highly porous interface material—the so-called Interfacial Transition Zone (ITZ)—which has important implications on the macroscale behaviour of concrete, both in terms of mass transport and deformational characteristics.

The SVEs were employed numerically using the the finite element method (FEM) to simulate mass transport—for both stationary and transient conditions—in order to compute macroscale diffusivities. Computations were carried out for various volume fractions of aggregates in the SVEs and for different diffusivities in the ITZ. For stationary conditions, the decrease in macroscale diffusivity attributed to increased volume fraction of aggregates was numerically determined. By use of the ITZ, the magnitude of this decrease in macroscale diffusivity could readily be controlled and altered. The influence of cracks on the macroscale diffusivity was also modelled and numerically evaluated. The numerical simulations showed that the macroscale diffusivity became anisotropic due to cracks and that the macroscale diffusivity rapidly increased in magnitude once cracks had begun to develop in the SVE.

This work forms a base for further modelling of the influence of mesoscale composition and cracking on the diffusivity of concrete, which has important implications for the durability of concrete structures.

Keywords: computational homogenization, mesoscale, statistical volume element, multiscale modelling, mass transport, coupled diffusion, interfacial transition zone.

Preface

The work constituting this thesis was carried out at the Division of Structural Engineering and the Division of Material and Computational Mechanics, at Chalmers University of Technology during 2009–2014. The research was financially supported by The Swedish Research Council (Vetenskapsrådet) which is gratefully acknowledged.

I thank my truly excellent supervisors Professor Karin Lundgren, Professor Fredrik Larsson and Professor Kenneth Runesson for all help, support and encouragement they have given me throughout these five years. They have—both individually and as a group—supervised me in the best possible way. This thesis would not have possible to write without them and they will always have my deepest respect.

I would also like to express my appreciation to all my fellow colleagues at the Division of Structural Engineering, the Division of Material and Computational Mechanics and the Division of Dynamics for creating such a nice working environment. I have had a really nice time at work thanks to them.

Lastly, I thank my family for all the support they have given me in my life and I thank my girlfriend Jacqueline for enriching my life in so many ways.

Göteborg, February 2014
Filip Nilenius

Thesis

This thesis consists of an extended summary and the following appended papers:

Paper A F. Nilenius, F. Larsson, K. Lundgren, and K. Runesson. "Macroscopic diffusivity in concrete determined by computational homogenization". In: *International Journal for Numerical and Analytical Methods in Geomechanics* 37.11 (Aug. 2013), pp. 1535–1551. ISSN: 03639061. DOI: 10.1002/nag.2097

Paper B F. Nilenius, F. Larsson, K. Lundgren, and K. Runesson. "An FE^2-method for coupled transient diffusion phenomena in concrete". In: *Journal of Engineering Mechanics* (2014). In press.

Paper C F. Nilenius, F. Larsson, K. Lundgren, and K. Runesson. "Computational homogenization of diffusion in three-phase mesoscale concrete". In: *Computation Mechanics* (2014). Accepted for publication.

Paper D F. Nilenius, F. Larsson, K. Lundgren, and K. Runesson. "Computational homogenization of crack-induced diffusivity in concrete". 2014. To be submitted for international publication.

Author's contribution to appended papers

The contributions of the present author to the appended papers are described below.

Paper A Responsible for planning and writing the paper. Adapted existing theories to coupled transport phenomena. Developed mesoscale model. Made numerical implementations and carried out numerical simulations.

Paper B Responsible for planning and writing the paper. Adapted existing theories to coupled transport phenomena. Developed mesoscale model. Made numerical implementations and carried out numerical simulations.

Paper C Responsible for planning and writing the paper. Developed mesoscale model. Made numerical implementations and carried out numerical simulations.

Paper D Responsible for planning and writing the paper. Developed mesoscale model. Made numerical implementations and carried out numerical simulations.

Other publications by the author

Conference proceedings

- F. Nilenius, F. Larsson, K. Lundgren, and K. Runesson. "A 3D/2D Comparison between Heterogeneous Mesoscale Models of Concrete". In: *Multi-Scale Modeling and Characterization of Infrastructure Materials*. Ed. by N. Kringos, B. Birgisson, D. Frost, and L. Wang. Vol. 8. RILEM Bookseries. Springer Netherlands, 2013, pp. 249–259. ISBN: 978-94-007-6877-2. DOI: 10.1007/978-94-007-6878-9_18.
- F. Nilenius, F. Larsson, K. Lundgren, and K. Runesson. "Determining effective diffusion properties of concrete through mesoscale analysis". In: *Proceedings of Microstructural-related Durability of Cementitious Composites*. Ed. by Y. Guang, K. van Breugel, W. Sun, and C. Miao. RILEM Publications s.a.r.l. 2012. ISBN: 978-2-35158-129-2.
- F. Nilenius, F. Larsson, K. Lundgren, and K. Runesson. "A multi-scale method for modeling of moisture and chloride ion transport in concrete". In: *Procceedings of XXI Nordic Concrete Research Symposium*. Ed. by T. nordic concrete federation. Vol. 43. 2011:1. Norsk betongforening. 2011, pp. 107–110. ISBN: 978-82-8208-025-5.
- F. Nilenius, F. Larsson, K. Lundgren, and K. Runesson. "Chloride transport in concrete modeled by the FE^2-method". In: *Proceedings of NSCM-23: the 23rd Nordic Seminar on Computational Mechanics*. Ed. by J. Freund and R. Kouhia. Vol. 24. 2011:23. Aalto University publication series. 2011. ISBN: 978-952-60-4347-0.
- F. Nilenius, F. Larsson, K. Lundgren, and K. Runesson. "Modeling of mass transfer in the microstructure of concrete: towards computational homogenization within a FE^2-strategy". In: *Proceedings of NSCM-23: the 23rd Nordic Seminar on Computational Mechanics*. Ed. by A. Eriksson and G. Tibert. Vol. 23. 2010:07. KTH Mechanics, Royal Institute of Technology. 2010, pp. 322–325.

Licentiate thesis

- F. Nilenius. "On Mesoscale Modelling of Coupled Chloride-Moisture Transport in Concrete". Licentiate Thesis. Chalmers University of Technology, 2011, p. 78.

Miscellaneous

- F. Nilenius, F. Larsson, K. Lundgren, and K. Runesson. "Tredimensionell modellering av betongens heterogena sammansättning". In: *Bygg & Teknik* 105.7 (Oct. 2013), pp. 56–59.

- F. Nilenius, F. Larsson, K. Lundgren, and K. Runesson. “Modellering och simulering av fukt- och kloridjonstransport i betongens mikrostruktur”. In: *Bygg & Teknik* 102.7 (Oct. 2010), pp. 50–54.

Contents

Notation

Acronyms

2D: two-dimensional
3D: three-dimensional
FE: finite element
FEM: the finite element method
HS$^+$: upper Hashin-Shtrikman bound
ITZ: Interfacial Transition Zone
RVE: Representative Volume Element
SVE: Statistical Volume Element

Nomenclature

Subscripts

a	aggregate
cp	cement paste
cr	crack
el	elastic
ITZ	Interfacial Transition Zone
I	largest eigenvalue

Greek letters

$\Gamma_\square$	boundary of SVE domain
κ	largest equivalent strain
ω	damage parameter
$\Omega_\square$	SVE domain
$\boldsymbol{\varepsilon}$	second order strain tensor
$\boldsymbol{\sigma}$	second order stress tensor
ϕ	moisture concentration

Roman lower case letters

$\bar{\boldsymbol{x}}$	centroid of SVE
c	chloride concentration
w_{cr}	crack width
t_{ITZ}	thickness of ITZ
$\boldsymbol{n}$	normal vector
h	element size
n_{a}	either area (2D) or volume (3D) fraction of aggregates

Miscellaneous

$\bar{\bullet}$	bar denotes macroscopic quantity
$\boldsymbol{\nabla}$	differential operator
$\langle\bullet\rangle_\square$	homogenized quantity
$\parallel$	parallel
$\perp$	perpendicular

Superscripts

M	macroscale
s	subscale

Roman capital letters

D	diffusion coefficient
$\boldsymbol{D}$	second order diffusivity tensor
$\boldsymbol{J}$	flux vector
$\mathbf{E}$	fourth order stiffness tensor
$\boldsymbol{I}$	second order unity tensor
A	surface area
E	Young's modulus
$L_\square$	side length of SVE
V	volume

Part I
Extended Summary

1 Introduction

1.1 Background

Concrete structures constitute a large and important part of the built environment, but they can severely deteriorate and lose functionality if exposed to aggressive substances such as chloride ions. Deterioration will induce loss in bearing capacity and can ultimately lead to structural collapse. Thus, controlling the ingress rate of chloride ions is an important aspect of the maintenance of concrete structures since the ingress of chloride ions impose high safety risks to the end users, e.g. motorists driving on a concrete bridge.

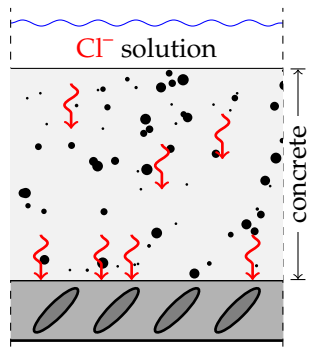

Figure 1.1: *Reinforcement bar (bottom) subjected to ingress of chloride ions (Cl^-).*

Chloride ions will initiate corrosion of embedded reinforcement bars if the ion concentration is sufficiently high. For a concrete structure subjected to constant loading, corrosion will yield higher tensile stresses in the reinforcement bars since the corrosion process reduces the cross sectional area of reinforcement bars. Additionally, the corrosion product will create tensile stresses in the concrete which may lead to spalling of the concrete cover, thereby making the reinforcement bars exposed to the ambient environment.

Typical sources of chloride ions are de-icing salts put on roads in winter times and salt dissolved in sea water. The dissolved ions will—through different transport mechanisms—migrate inwards from the surface of the concrete structure to the embedded reinforcement bars, cf. Figure 1.1.

Hence, it becomes important to predict chloride ion ingress and to understand the parameters that govern the ingress mechanisms because such predictions and understanding allow for a time estimate of possible corrosion initiation. In addition, chloride ingress interacts with moisture transport; therefore, the moisture conditions need to be considered as well for improved time prediction.

Concrete is a strongly heterogeneous material on the mesoscale and the chloride ingress rate will depend on its heterogeneous composition. Computational homogenization—within a multiscale modelling framework—provides a method to numerically homogenize such material heterogeneities to obtain up-scaled material properties while keeping computation cost at a moderate level. Instead of having to

fully resolve the heterogeneous structure of the material, only a so-called Statistical Volume Element (SVE) of the subscale morphology is modelled for which numerical work is carried out. By this procedure, only the SVE needs to be fully resolved and the computational cost can, therefore, be reduced by several orders of magnitude. The SVE will in this setting provide a constitutive model for the macroscale response.

1.2 Aim of research

The aim of this research was to develop and implement a multiscale model of heterogeneous concrete and to utilize the model for computational homogenization of transport phenomena in concrete. In particular, the transport of (coupled) moisture and chloride diffusion was to be considered for both stationary and transient conditions.

More specifically, an SVE of concrete would be developed to be able to account for the heterogeneous mesoscale structure of concrete as well as the intrinsically non-linear material properties of the mesoscale constituents. The SVE would be used to numerically investigate how the mesoscale structure and composition influence the mass transport in concrete on the macroscale.

1.3 Methodology and scientific approach

The methodology used in this work was (*i*) to study and learn about transport phenomena in concrete from a physical standpoint and discover the key factors influencing these phenomena, (*ii*) to review the state-of-the-art in terms of mathematical modelling of transport phenomena in concrete, and (*iii*) to develop and implement numerical models of concrete in conjunction with methods of computational homogenization in order to simulate chloride and moisture transport in concrete.

Tasks (*i*) and (*ii*) were mainly conducted through literature reviews and specific subject courses—given by various universities and organisations—to provide necessary context to the research. The scientific problem of task (*iii*) was to numerically model and simulate (coupled) transport of moisture and chloride ions in concrete on the mesoscale level by means of computational homogenization. This task was accomplished by the development of a set of computer programs. All numerical implementation was done in MATLAB [43], and all source code was written by the author, with the exception of a few function files pertaining to the CALFEM package [4].

1.4 Scope and limitations

Throughout this work, it was assumed that the mass transfer of chloride ions and moisture are concentration gradient-driven processes, allowing for Fick's law to be used. Hence, convection was assumed to be embedded in the diffusion process and the migration of chloride ions was considered small.

The thesis has been restricted to homogenization of the mesoscale in which concrete was considered a mixture of cement paste, aggregates, cracks and the Interfacial

Transition Zone (ITZ). Subscales below the mesoscale have not been considered. The mesoscale constituents were assumed to be homogeneous, and the laws of continuum physics were assumed to apply at the mesoscale level.

First order homogenization—based on the assumption that the macroscale fields of moisture and chloride ions vary linearly within the SVE—was adopted consistently. This assumption pertains to the lowest order coupling between the fields and is valid in the limit of complete separation of scales.

Only Dirichlet boundary conditions have been used in the numerical implementations and all numerical results are—as a consequence—upper bound solutions. Corresponding lower bound solutions—obtained by the use of Neumann boundary conditions—have not been considered in this study.

1.5 Significance of research

As explained in Section 1.1, the ingress of chloride ions in concrete causes concrete structures to lose their load-carrying capacity. As a result, expensive repair work is required. To better be able to model and predict such ion ingress therefore becomes important, and much research has indeed been devoted to this topic.

However, the strongly heterogeneous structure of concrete influences the ingress rate, which is a process that poses modelling difficulties. To assess the effects the heterogeneities have on the chloride ion and moisture ingress rates is still an open problem, and more work in this research field is therefore needed.

Additionally, the method of computational homogenization is currently more often applied in the context of mechanical problems. Corresponding work for transport phenomena and mass transfer is less frequently found in the literature; hence, knowledge in this research area will hopefully increase as a result of this thesis.

2 Transport mechanisms in concrete

2.1 Preliminaries

This section provides a summary of the various transport mechanisms related to moisture and chloride transport in concrete. Comprehensive literature on this subject can be found in the work by Černý and Rovnaníková [14] (concrete specific) and in the classical work by Bird et al. [9] (generic mass transport). First, a brief introduction to the composition of concrete is provided for completeness. Comprehensive literature on this topic can be found in the work by Mehta and Monteiro [44].

2.2 Concrete composition

Concrete is a highly complex composite material since it is a mixture of cement, aggregates (typically gravel), and additional admixtures merged together through multiple chemical processes, cf. Figure 2.1. Cement is in turn a composite material as it is made up of clinkers (limestone and clay) and grounded gypsum.

Figure 2.1: *Mesoscale structure of concrete. The heterogeneous and random structure of the material is evident and affects the macroscopic material behaviour. The porosity of the cement paste is also observable in this photo.*

Hydrated cement is a porous substance made up of primarily four solid phases: calcium silicate hydrate (H_2CaO_4Si), calcium hydroxide ($Ca(OH)_2$), calcium sulfoaluminate hydrates ($C_6AS_3H_{32}$ and C_4ASH_{18}) and unhydrated clinker grains (C_3S, C_2S, C_3A and C_4AF). It is the porosity of the cement paste, the ITZ and cracks that enable mass transport in concrete.

As the hydration process advances over long periods of time, the mechanical and physical properties of concrete change as the material matures and hardens. Consequently, the composition of concrete varies in space and time in an intricate manner and many factors contribute to the physical and mechanical properties of concrete.

The aggregates can be of varying type and shape and provide stiffness and functions as a filler to the cement paste. The contact zone between the cement paste and aggregates—measured in the range of micrometers (µm)—is commonly referred to as the Interfacial Transition Zone (ITZ) and is characterized by low stiffness and high diffusivity.

2.3 Moisture transport

For saturated[1] conditions, pressure gradients are the main driving forces for moisture transport. For unsaturated conditions, moisture exists simultaneously in two phases[2] as liquid and as vapour. The driving forces for the liquid phase are pressure gradients in addition to capillary forces. For the vapour phase, diffusion and convection are the two main transport mechanisms. It may be difficult to distinguish between the above listed transport mechanisms in an experimental environment; depending on the degrees of moisture saturation, these mechanisms often act in combination with each other.

[1] all cement pores completely filled with water in liquid phase.
[2] assuming non-freezing conditions.

Moisture diffusivity of unsaturated concrete was early on expressed by Bažant and Najjar [7] as a non-linear function of pore humidity and their proposed analytical model was in the same work calibrated with experimental data. Xi et al. [70] later extended this model to include moisture capacity—as a function of water-cement ratio, curing time, temperature and type of cement—as the derivative of the adsorption isotherm. Vanderheijden et al. [64] did experimental work on the effect of temperature on moisture transport and Poyet [53] did the corresponding numerical modelling.

2.4 Chloride transport

Chlorides are solved only in the liquid phase of moisture, not in the vapour phase. This phenomenon makes the transport of chloride ions intrinsically coupled to the transport of moisture. The three main transport processes are diffusion, convection and migration. As the ions are electrically charged, they will move with electric currents, a phenomenon commonly referred to as migration. As with moisture, the various transport processes can be difficult to differentiate between, and it is common to apply a constitutive model assumed to capture all different transport types combined (as done in this work).

Tang and Nilsson [61] proposed a method for evaluating the chloride binding capacity of concrete and suggested that the relationship between free and bound chlorides could be described by the Freundlich isotherm. In [62], the same authors established a relationship between the diffusivity and pore size distribution of hardened cement paste. Xi and Bažant [69] modelled chloride ingress in saturated concrete whereas Delagrave et al. [16] and Halamickova et al. [29] studied the influence of ITZ on chloride diffusivity. Johannesson [31–33] developed theoretical transport models of chloride ions and moisture in concrete which were numerically evaluated using FEM. Wang et al. [66] modelled chloride ingress from a saline environment, Koniorczyk and Wojciechowski [37] modelled the influence of salt on the moisture isotherm and concluded that salt has great influence on moisture capacity. Li et al. [40] computed effective chloride diffusivities using two- and three dimensional heterogeneous models of concrete and concluded that the aggregate shape has small influence on the diffusivity.

The coupled action of chloride ion and moisture transport has been studied and modelled by several authors including Halamickova et al. [29], Ababneh et al. [1], Černý [13], Puatatsananon and Saouma [54], Suwito et al. [60] and Baroghel-Bouny et al. [5]. At the Chalmers University of Technology, the research on chloride ion transport and its subsequent reinforcement corrosion has resulted in several PhD theses, e.g. Lindvall [42], Zandi Hanjari [73] and Silva [57].

In this thesis, the coupled interaction between chloride ions and moisture has been modelled for both stationary and transient conditions in **Paper A** and **Paper B**, respectively. The constitutive model developed by Ababneh and Xi [2] was used for the cement paste, which cross-couples the fluxes of chloride ions and moisture in the following way:

$$\boldsymbol{J}_{\phi} = -D_{\phi}\boldsymbol{\nabla}\phi - \varepsilon_{\mathrm{c}} D_{\mathrm{c}}\boldsymbol{\nabla} c, \tag{2.4.1}$$

$$\boldsymbol{J}_{\mathrm{c}} = -\varepsilon_{\phi} D_{\phi}\boldsymbol{\nabla}\phi - D_{\mathrm{c}}\boldsymbol{\nabla} c, \tag{2.4.2}$$

where ϕ and c represent the relative pore humidity and free chloride ion concentration, respectively, and $\boldsymbol{\nabla}$ the nabla operator. Flux is denoted $\boldsymbol{J}_{\bullet}$ and $D_{\bullet}$ denotes the diffusion coefficient. This constitutive model can be seen as a modified expression of Fick's law where the numerical value of each coupling parameter $\varepsilon_{\bullet}$ determines the degree to which the fluxes of chloride ions and moisture are coupled.

In **Papers C** and **D**, the coupled interaction was not considered in favour of more generic mass transport, and focus was shifted towards material modelling in terms of morphology material cracking.

3 Computational homogenization

3.1 Introduction

The physical and mechanical properties of a material, measured on any given scale, represent the combined properties of the underlying subscale features of the material. For instance, the measured macroscopic transport properties of concrete are expected to depend on such factors as the aggregate content and porosity of the cement paste, both of which are subscale material constituents. Consequently, if the features of the subscale vary within the material, the measured property will vary accordingly.

Homogenization techniques strive to derive equivalent homogeneous properties of a heterogeneous material. Analytical homogenization methods date back to early 1887 (Voigt) and 1929 (Reuss) for two-phase composite materials. In recent years, the interest in computational homogenization techniques, in conjunction with multiscale methods, has grown as a result of the continuously increasing computational power provided by computers. This enables the finite element method (FEM), cf. Bathe [6] and Zienkiewicz and Taylor [74], to be employed since computational homogenization techniques require numerical solutions to the governing balance equations of either momentum, mass or energy. Numerical techniques make it possible to study complex materials both in terms of geometry and interface descriptions as well as problems of non-linear material behaviour. Additionally, randomness in material structure can be accounted for in a straight-forward manner using numerical techniques.

Early work on computational homogenization include e.g. the work of Fish et al. [19], Miehe et al. [45], and Nemat-Nasser and Hori [46] related to problems of elasticity and plasticity. Work on nested two-scale homogenization—so-called FE^2— has been carried out by e.g. Feyel and Chaboche [18], Kouznetsova et al. [38], Özdemir et al. [52], Larsson et al. [39] and Su et al. [59] dealing with various problems of plasticity, transient heat flow and coupled problems of consolidation. Additional selected references on

computational homogenization are the works of Terada [63], Kalidindi et al. [34], Baroghel-Bouny et al. [5] and Ngoc et al. [47], Wellmann et al. [67] and De Lorenzis and Wriggers [15]. The work by Geers et al. [23] provides a discussion on trends and developments on multiscale computational homogenization with further references.

Some selected references on computational homogenization applied to concrete include Gal and Kryvoruk [20] who proposed a two-step homogenization procedure to determine elastic properties of fiber reinforced concrete. Computational homogenization was used by Nguyen et al. [48] to model calcium leaching in concrete, in addition to Hain and Wriggers [27, 28] and Wriggers and Moftah [68] who modelled elastic properties and damage in hardened cement paste. Early work on homogenization and numerical techniques applied to cement paste can be found in the work by Garboczi [21] and Garboczi and Bentz [22].

3.2 Methodology

A classical method by which heterogeneous materials may be modelled is through phenomenology. Phenomenological models are typically calibrated with experimental data by use of model parameters. Such models can be of varying complexity depending on the physical behaviour they try to describe. Quite significantly, the model parameters might lack physical interpretation since they mainly serve to curve fit an analytical function to a set of experimentally obtained data points.

Computational homogenization uses a different approach and Fick's law of diffusion is used as an example to show the principle of this method: Fick's law states that

$$\bar{\boldsymbol{J}} = -\bar{\boldsymbol{D}} \cdot \bar{\boldsymbol{\nabla}}\bar{\phi}, \tag{3.2.1}$$

where $\bar{\boldsymbol{J}}$ represents the macroscale flux, and $\bar{\boldsymbol{\nabla}}\bar{\phi}$ the macroscale moisture gradient. $\bar{\boldsymbol{D}} = \bar{\boldsymbol{D}}(\alpha, \beta, ...)$ represents the effective material diffusivity—i.e. the diffusivity of concrete—which may depend on a number of subscale parameters, $\alpha, \beta, ...$ The approach used in phenomenology is to determine the diffusivity of concrete by experimentally calibrating $\bar{\boldsymbol{D}}$ using a set of test specimens of varying types of concrete.

Now, let $\boldsymbol{D}_{\text{cp}}$ and $\boldsymbol{D}_{\text{a}}$ denote the intrinsic diffusivity of the cement paste and aggregates, respectively. The approach used in computational homogenization is instead to experimentally determine the diffusivities of cement paste and aggregates separately, after which these two values are computationally homogenized to obtain the diffusivity of concrete, i.e.

$$\bar{\boldsymbol{D}} = \bar{\boldsymbol{D}}(\boldsymbol{D}_{\text{cp}}, \boldsymbol{D}_{\text{a}}), \tag{3.2.2}$$

thus removing the need for α and β, both of which may have no physical interpretation. In this way, the experimental measurements required would instead be carried out on a finer subscale and the macroscopic material property would be obtained solely as a result of computation. In practice, Eq. (3.2.2) is obtained using computational homogenization by solving a boundary valued problem on a set of Statistical Volume Elements (SVEs), as defined in Section 3.4.

Alternatively, if $\boldsymbol{D}_{\text{cp}}$ would be difficult to determine experimentally—$\boldsymbol{D}_{\text{cp}}$ might also depend on a number of subscale parameters $\alpha_{\text{cp}}, \beta_{\text{cp}}, ...$—computational homogenization could also be used to solve the inverse problem of calibrating $\boldsymbol{D}_{\text{cp}}$ from experimental data of $\bar{\boldsymbol{D}}$.

The overall goal of this procedure is to reduce the number of experimentally obtained macroscopic constitutive models needed, and have them replaced by constitutive models which are physically sounder and applied on a finer length scale. Additionally, it is cheaper and less time consuming to obtain Eq. (3.2.2) computationally than through experiments.

3.3 Multiscale formulation and first order homogenization

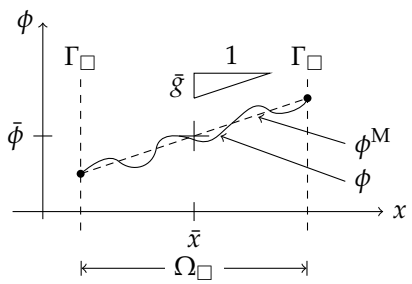

Figure 3.1: *1D illustration of ϕ^M and its linear variations within the SVE domain $\Omega_\square$.*

The basic starting-point of the multiscale formulation is the formal splitting of the scalar field ϕ in an additive manner as

$$\phi = \phi^{\text{M}} + \phi^{\text{s}}, \tag{3.3.1}$$

corresponding to the macroscale part ϕ^{M} and subscale part ϕ^{s} which contains the fluctuations of the total scalar field. It is further assumed that $\phi = \phi^{\text{M}}$ on the boundary of the SVE, $\Gamma_\square$; hence, $\phi^{\text{s}} = 0$ on $\Gamma_\square$.

First order homogenization pertains to the assumption that ϕ^{M} varies linearly within the SVE, cf. Figure 3.1, which yields the representation

$$\phi^{\text{M}}(\boldsymbol{x}, \bar{\boldsymbol{x}}) = \bar{\phi}(\bar{\boldsymbol{x}}) + \bar{\boldsymbol{g}}(\bar{\boldsymbol{x}}) \cdot [\boldsymbol{x} - \bar{\boldsymbol{x}}] \quad \forall \boldsymbol{x} \in \Omega_\square, \tag{3.3.2}$$

where $\bar{\boldsymbol{x}}$ is the centroid of the SVE and

$$\bar{\boldsymbol{g}}(\bar{\boldsymbol{x}}) \stackrel{\text{def}}{=} (\boldsymbol{\nabla}\bar{\phi})(\bar{\boldsymbol{x}}). \tag{3.3.3}$$

In case of stationary conditions, mass balance on the fine scale is stated as

$$\boldsymbol{\nabla} \cdot \boldsymbol{J} = 0 \quad \text{in } \Omega, \tag{3.3.4}$$

where $\boldsymbol{J}$ is the flux, $\boldsymbol{\nabla}$ is the nabla operator and $\Omega \in \mathbb{R}^3$ is the domain where all material heterogeneities are embedded. By utilizing the split of the scalar field in Eq. (3.3.1) and the method of first order homogenization, the macroscale flux $\bar{\boldsymbol{J}}$ can be identified[1] as the volume average of the flux in the SVE, i.e.

$$\bar{\boldsymbol{J}} = \langle \boldsymbol{J} \rangle_\square, \tag{3.3.5}$$

[1] derivations omitted here but can be found in the appended papers.

where the homogenized quantity $\langle \boldsymbol{J} \rangle_\square$ of $\boldsymbol{J}(\boldsymbol{x})$ is defined as the volume average:

$$\langle \boldsymbol{J} \rangle_\square \overset{\text{def}}{=} \frac{1}{|\Omega_\square|} \int_{\Omega_\square} \boldsymbol{J}(\boldsymbol{x}) \, \mathrm{d}\Omega_\square, \tag{3.3.6}$$

where $\Omega_\square$ denotes the domain occupied by the Statistical Volume Element (SVE)—which is defined in the following subsection. Once the macroscale flux is computed for a given macroscale gradient of either moisture of chloride ions, the macroscale diffusivity can be determined from Eq. (3.2.1).

Macroscale diffusivities are in **Papers A**, **C** and **D** determined by means of *a priori* homogenization, i.e. when the subscale material properties are assumed to be linear. **Paper B** considers the case of non-linear subscale material properties and employs a nested FE^2-algorithm where the SVE is introduced in the Gauss points of the macroscale domain.

3.4 Statistical Volume Element (SVE)

Central to computational homogenization is the concept of a Statistical Volume Element (SVE). The SVE should in a statistical manner represent the subscale morphology of the material as accurately as possible. Additionally, for materials with random structure—such as concrete—it is essential to have multiple SVE realizations to capture statistical scatter in numerical results.

Closely related to the notion of an SVE is the Representative Volume Element (RVE). An SVE is said to become an RVE only when it is sufficiently large such that any boundary effect is negligible. For materials with random structure, a true RVE is never obtained in practice but can only be approximated by a finite set of SVE realizations, cf. Figure 3.2. A quantitative prediction of how to obtain a sufficiently large RVE is proposed in the work by Kanit et al. [35] and the distinctions between SVEs and RVEs is further discussed by Ostoja-Starzewski [51]. The SVE models developed in this work are introduced in Section 4.

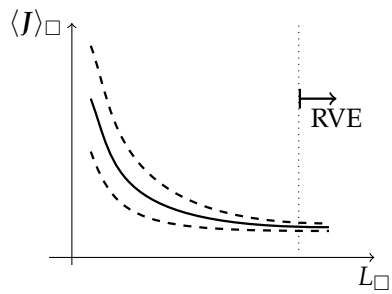

Figure 3.2: *Homogenized flux as a function of SVE size, $L_\square$, in terms of mean values (solid line) and statistical spread (dashed lines) for multiple SVE realizations. An RVE is said to have been obtained when the mean value has converged and the statistical spread is sufficiently small.*

4 Mesoscale models of concrete

4.1 Preliminaries

Concrete possesses strong heterogeneities on multiple length scales, as indicated in Section 2.2. On the mesoscale, the heterogeneities mainly stem from the inclusion of aggregates and the Interfacial Transition Zone (ITZ) in the cement paste. The ITZ is a highly porous and thin phase of the cement paste that constitutes the interface between the aggregate particles and the bulk cement paste. The high porosity of the ITZ yields higher diffusivity and lower stiffness than the bulk cement paste. Two- and three-dimensional SVEs was developed to mimic the heterogeneous morphology and are described below. Two-dimensional mesoscale representations of concrete were developed and used in **Papers A** and **B**. In **Papers C** and **D**, the mesoscale representation was extended to include all three spatial dimensions.

4.2 Algorithm for generating Statistical Volume Elements

An algorithm to generate SVEs was developed, implemented and utilized in the appended papers, see Algorithm 1. The algorithm will run until the desired aggregate content has been reached and is constructed such that no aggregates will overlap. The numerical implementation of Algorithm 1 allows the input of different aggregate sizes as a sieve curve in which each aggregate size has its own volume fraction. Two sets of SVE realizations produced by the algorithm is shown in Figures 4.1 and 4.2.

Algorithm 1 Algorithm to generate SVEs.

```
while the volume fraction of aggregates inside SVE is smaller than desired do
    generate aggregate from given sieve curve.
    place the new aggregate at a random point in Ω_□.
    if new particle overlaps already existing particle then
        remove the new aggregate.
    end if
    add area/volume of the new aggregate to the accumulated aggregate area/volume.
end while
```

4.3 Aggregate representation and FE discretization

2D SVEs In 2D, the aggregate representation was based on octagons and the randomness in shape of the aggregate was rendered by adding a random variation to each corner point in the octagon. The finite element discretization was carried out using a Delaunay triangulation algorithm. Similar techniques using Voronoi tesselation was in

early work by Roelfstra et al. [55] and Stankowski [58] utilized to numerically generate a two-dimensional heterogeneous structure and the same method was utilized—combined with lattice elements—by e.g. Schlangen and Mier [56], Grassl and Rempling [26], Grassl [24], Idiart et al. [30] and Wang and Ueda [65] to model mechanical problems related to fracture and damage, as well as problems of moisture transport.

The main advantage of a 2D model is its relatively low computational cost. The main drawback is that the heterogeneities—in terms of aggregates—adopt shapes similar to bars in the out-of-plane direction.

3D SVEs In 3D, the aggregates were modelled as spheres. In contrast to the 2D representation, no random variation in shape was applied. The spatial discretization technique was based on voxelization to create a structured grid of identically sized voxels (cubes). The concept is to subdivide the continuous SVE into a discrete set of voxels which are considered solid finite elements.

The same voxelization approach was used by Bentz et al. [8] and Garboczi [21] in the context of analytical homogenization of heterogeneous concrete and later adapted by Hain and Wriggers [27, 28] for elasticity problems and computational homogenization. Voronoi tesselation was also used in 3D by Asahina and Bolander [3], Caballero et al. [11], and Carol et al. [12] whereby the aggregates were based on a polyhedron representation. Lattice elements were used in 3D by Grassl and Davies [25] and Lilliu and Mier [41] to model corrosion induced cracking and fracture processes, respectively.

The main advantage of a 3D model is that it is possible to obtain a more realistic representation of the morophology of the material. An obvious drawback is the higher computational cost compared to 2D models. However, the relatively higher computational cost is likely to be of less significance in the future if Moore's law[1] can be assumed to hold.

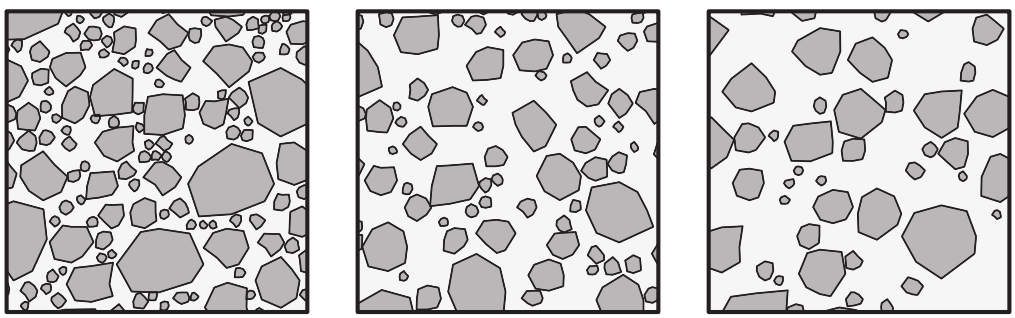

(a) $L_\square = 8\,\text{cm}$, $n_\text{a} \approx 0.6$. (b) $L_\square = 8\,\text{cm}$, $n_\text{a} \approx 0.5$. (c) $L_\square = 8\,\text{cm}$, $n_\text{a} \approx 0.4$.

Figure 4.1: *2D SVE realizations with varying aggregate content generated by Algorithm 1. These SVEs are generated from the same sieve curve. Area fraction of aggregates is denoted* n_a.

[1] Moore's law states that the number of transistors on integrated circuits doubles approximately every two years.

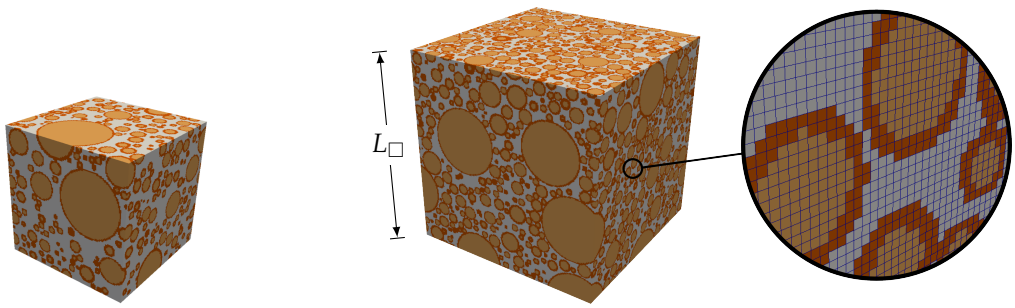

(a) $L_\square = 4\,\text{cm}$, $n_\text{a} \approx 0.4$.

(b) $L_\square = 6\,\text{cm}$, $n_\text{a} \approx 0.6$. *The circular figure shows the FE discretization.*

Figure 4.2: *3D SVE realizations with varying sizes and aggregate content generated by Algorithm 1. These SVEs are generated from the same sieve curve. Volume fraction of aggregates is denoted n_a and $L_\square$ denotes the side length of the SVE.*

4.4 Constitutive relations for the mesoscale materials

Fick's law was used consistently to model mass flux on the mesoscale level and different diffusion coefficients were assigned to the mesoscale constituents.

Cement paste The following, non-linear, expressions for moisture diffusivity, D_ϕ, and chloride diffusivity, D_c, were used in **Paper A** and **Paper B**

$$D_\phi(\phi) = \alpha_h + \beta_h \left[1 - 2^{-10^{\gamma_h[\phi-1]}}\right] \qquad [\text{cm}^2/\text{day}], \tag{4.4.1}$$

$$D_\text{c}(\phi, c) = f_1(t_0) f_2(n_\text{a}) f_3(\phi) f_4(T) f_5(c) \qquad [\text{cm}^2/\text{day}], \tag{4.4.2}$$

A detailed description of these expressions are found in Xi and Bažant [69] and Xi et al. [70]. In **Paper C** and **Paper D**, a constant diffusivity were used equal to unity.

Aggregates A diffusivity equal to zero was used in all papers.

Interfacial Transition Zone (ITZ) The ITZ implementation made the ITZ diffusivity a model parameter and different values were used to study the influence on the macroscopic diffusivity, cf. Section 4.5 below.

4.5 Implementation of the Interfacial Transition Zone (ITZ)

Different strategies to account for the effects of the ITZ have been devised in the literature: Wang and Ueda [65] used lattice elements to model the effects of ITZ whereas Kim and Al-rub [36] chose to fully resolve the ITZ in the FE mesh. Much experimental

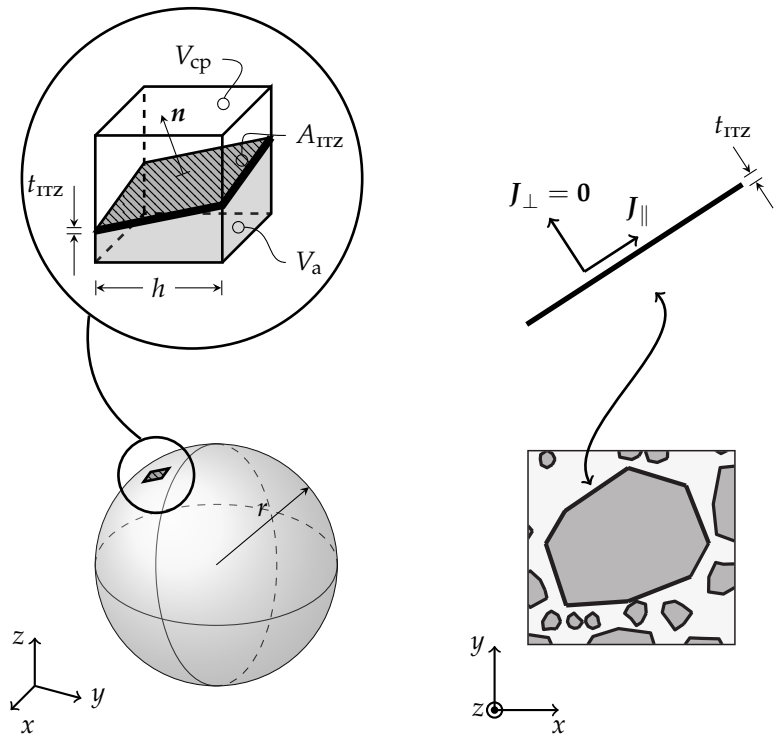

(a) *3D implementation of the ITZ. Interface voxel (upper) located on the surface of a spherical aggregate (lower). Nodes only exist at the corners of the voxel.*

(b) *2D implementation of the ITZ. Nodes are introduced at both ends of each ITZ line segment. The flux parallel to the length direction is denoted $\boldsymbol{J}_\parallel$ and $\boldsymbol{J}_\perp$ is the perpendicular flux, which is zero by construction.*

Figure 4.3: *ITZ, as introduced on the mesoscale in 2D and 3D. In 3D, the ITZ is imposted by element rule of mixture of the Voigt type, whereas in 2D the ITZ is imposted by a separate 1D element along the boundary of each aggregate. The thickness of the ITZ, t_{ITZ}, is no geometrical property but only a parameter in the constitutive material models.*

work has been carried out to measure the influence the ITZ has on the physical and mechanical properties of concrete and the general conclusion is that the ITZ significantly enhances diffusivity and weakens concrete subjected to mechanical loading, cf. Nilsen and Monteiro [49], Ollivier et al. [50], Diamond and Huang [17], Yang and Cho [71] and Yang and Cho [72], and Buenfeld et al. [10].

Diffusivity in 2D SVEs The ITZ was introduced as a 1D continuum on the mesoscale, modelling additional[2] flux along the interface between the cement paste and each aggregate particle. The main characteristic of the ITZ implementation is that diffusion is only allowed in its own length direction. Figure 4.3b shows how the ITZ was introduced in the 2D mesoscale model.

Diffusivity in 3D SVEs The ITZ was not modelled by individual elements, instead the effect of the ITZ was included in the finite elements which contained the aggregate boundaries, cf. Figure 4.3a. The ITZ was here implemented using analytical averaging of Voigt type:

$$\boldsymbol{D}_{\text{ITZ}} = \frac{V_{\text{a}} D_{\text{a}} + V_{\text{cp}} D_{\text{cp}}}{h^3} \boldsymbol{I} + \frac{A_{\text{ITZ}} D_{\text{ITZ}} t_{\text{ITZ}}}{h^3} \left(\boldsymbol{I} - \boldsymbol{n} \otimes \boldsymbol{n} \right), \tag{4.5.1}$$

where $D_\bullet$ are diffusivity coefficients[3], $V_\bullet$ are volumes [cm^3] of aggregate and cement paste, $\boldsymbol{n}$ and A_{ITZ} is the normal and area [cm^2], respectively, of the ITZ as shown in Figure 4.3a. By this formulation, the diffusivity tensor $\boldsymbol{D}_{\text{ITZ}}$ becomes anisotropic due to its dependence of the surface normal, $\boldsymbol{n}$.

Elasticity in 3D SVEs The elastic properties of the ITZ were modelled to be transversal isotropic where the surface of the ITZ constitutes the plane of isotropy. The in-plane Young's modulus, E_{P}, was computed using Voigt's rule of mixture

$$E_{\text{P}} = \frac{1}{h^3} (V_{\text{a}} E_{\text{a}} + V_{\text{cp}} E_{\text{cp}} + A_{\text{ITZ}} t_{\text{ITZ}} E_{\text{ITZ}}), \tag{4.5.2}$$

and Young's modulus in the transversal direction, E_{T}, was computed using Reuss' rule of mixture

$$\frac{h^3}{E_{\text{T}}} = \frac{V_{\text{a}}}{E_{\text{a}}} + \frac{V_{\text{cp}}}{E_{\text{cp}}} + \frac{A_{\text{ITZ}} t_{\text{ITZ}}}{E_{\text{ITZ}}}, \tag{4.5.3}$$

where h is the element size, cf. Figure 4.3a, and E_{ITZ} is the Young's modulus of ITZ which is assumed to be a scaled value of E_{cp} on the form

$$E_{\text{ITZ}} = \alpha E_{\text{cp}}, \quad \text{where } \alpha \in (0, 1). \tag{4.5.4}$$

[2] note that in this framework, the 1D ITZ-material is superimposed on the interface.
[3] a = aggregate, cp = cement paste.

By Eq. (4.5.3), E_{T} will approximately equal E_{ITZ} for a sufficiently large A_{ITZ}. The motivation for this formulation is that the ITZ constitutes a weak zone in concrete through which cracks tend to propagate. The stiffness in the transversal direction should, therefore, be governed by the stiffness of the ITZ to capture this effect. Furthermore, the elastic strain will tend to be concentrated in the ITZ, initiating the development of cracks. However, since the third term on the right hand side of Eq. (4.5.2) will be much smaller in magnitude than the other two, in the plane of isotropy, the stiffness will be governed by the stiffness of cement paste and aggregate. Effectively, the ITZ will only influence, i.e. reduce, the element stiffness in the transverse direction.

4.6 Crack modelling

Cracks were modelled in **Paper D** by means of an isotropic damage model on the form

$$\boldsymbol{\sigma} = (1-\omega)\mathbf{E} : \boldsymbol{\varepsilon}, \tag{4.6.1}$$

$$\omega = g(\kappa), \tag{4.6.2}$$

where ω is a scalar damage parameter and κ is a scalar measure of equivalent strain. Once damage was initiated in an element, the crack was assumed to be perpendicular to the largest principal strain direction $\boldsymbol{n}_{\mathrm{I}}$, cf. Figure 4.4. The diffusivity of a cracked element is expressed on the form

$$\boldsymbol{D}_{\mathrm{cr}} = \boldsymbol{D}_{\mathrm{cp}} + \frac{A_{\mathrm{cr}} D_{\mathrm{cr}} w_{\mathrm{cr}}}{h^3} \left(\boldsymbol{I} - \boldsymbol{n}_{\mathrm{I}} \otimes \boldsymbol{n}_{\mathrm{I}} \right), \tag{4.6.3}$$

which is analogous to Eq. (4.5.1). The parameters in Eq. (4.6.3) are defined in Figure 4.4. The crack width, w_{cr}, was computed from the expression

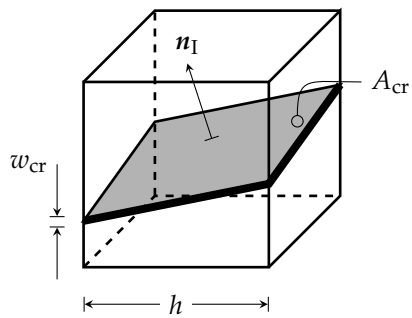

Figure 4.4: *Damaged finite element with a crack plane perpendicular to $\boldsymbol{n}_I$ with an associated crack area A_{cr}. The crack plane is assumed to be perpendicular to the largest principal strain direction, $\boldsymbol{n}_I$.*

$$w_{\mathrm{cr}} = h\boldsymbol{n}_{\mathrm{I}} \cdot [\boldsymbol{\varepsilon} - \underbrace{\mathbf{E}^{-1} : \boldsymbol{\sigma}}_{\boldsymbol{\varepsilon}_{\mathrm{el}} = (1-\omega)\boldsymbol{\varepsilon}}] \cdot \boldsymbol{n}_{\mathrm{I}} = h\omega\varepsilon_{\mathrm{I}}. \tag{4.6.4}$$

In the numerical simulations, A_{cr} was computed for each damaged finite element since the value would depend directly on the orientation of the principal strain direction $\boldsymbol{n}_{\mathrm{I}}$.

5 Summary of appended papers

On the basis of the previous discussion of transport mechanisms, computational homogenization and mesoscale modelling of concrete, a model framework was developed and implemented for numerical analyses. The appended papers constitute documentation of this work, and the contents of each paper is here briefly summarized.

Paper A: "Macroscopic diffusivity in concrete determined by computational homogenization"

Macroscopic moisture and chloride ion diffusivity of concrete was in this paper determined by means of computational homogenization. In particular, the dependence of the aggregate content on the macroscopic diffusivity was established. Computational results show that the macroscopic diffusivity obtained is in agreement with the upper Hashin-Shtrikman bound.

Furthermore, the influence of ITZ on the macroscopic diffusivity was studied. The diffusion coefficient of the ITZ was calibrated using experimental data and the results show that the ITZ has a considerable effect on macroscopic diffusivity, cf. Figure 5.1.

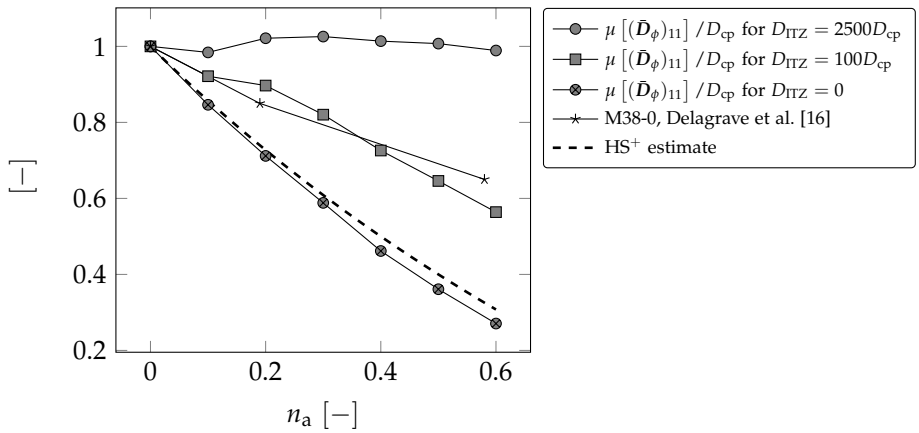

Figure 5.1: *Main computational results from **Paper A**. Normalized effective diffusivities as a function of aggregate contents for varying diffusivities in the ITZ. Area fraction of aggregates is denoted* n_a.

Paper B: "An FE^2-method for coupled transient diffusion phenomena in concrete"

Transient simulations of coupled moisture-chloride diffusion in concrete were carried out using an FE^2-algorithm. Using this procedure, the diffusion of moisture and chloride was studied on the macroscale for various concrete compositions on the mesoscale.

Computational results show that the aggregate content has a versatile effect on the macroscale behaviour. An increase in the aggregate content both increases and decreases the diffusion rate, depending on the location in the macroscale domain. Furthermore, the aggregate content influences the diffusion of moisture and chloride differently. This behaviour is expected to be due to different relations between conservation properties and the diffusivities of moisture and chloride. Computational results from **Paper B** are shown in Figures 5.2 and 5.3 below.

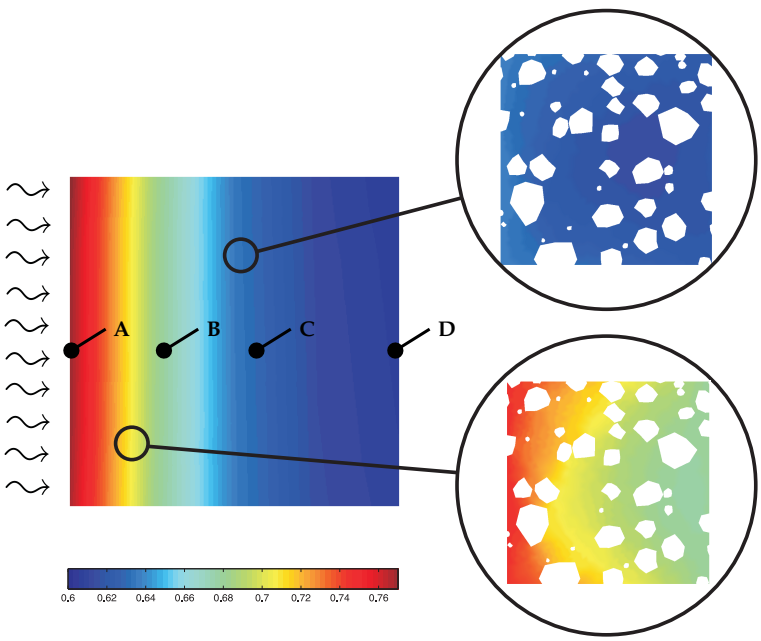

Figure 5.2: *Snapshot of transient solution from the FE^2-algorithm. The smooth solution on the macroscale (left) is obtained by homogenizing the non-smooth RVE responses (right).*

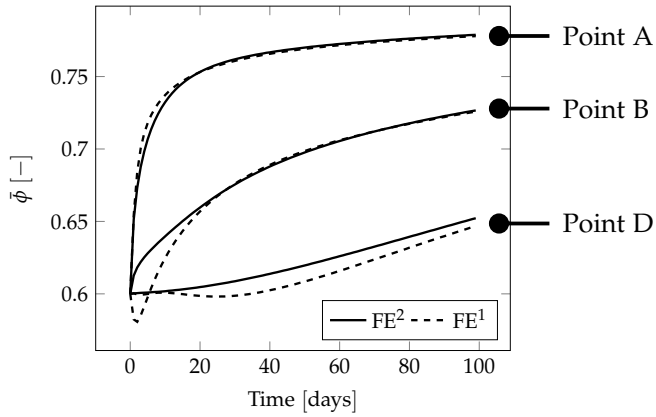

Figure 5.3: *Time evolution of macroscale relative humidity, $\bar{\phi}$, for the different schemes, FE^2-and FE^1 (conventional FE-modeling) where $n_a = 0\,\%$ for both models. The initial relative humidity is 0.6 % and ambient relative humidity is 0.8 %. Early in the simulation, the FE^2-algorithm yields more stable results since the results obtained from the conventional FE-modelling (FE^1) are below the initial condition. Points A,B and D are defined in Figure 5.2.*

Paper C: "Computational homogenization of diffusion in three-phase mesoscale concrete"

A three-dimensional SVE of concrete was in this paper developed and employed for homogenization of mass diffusion on the mesoscale. An RVE was approximated from convergence studies of SVEs of different sizes and parametric studies were carried out with respect to aggregate content and ITZ diffusivity.

Computations were carried out on both two- and three-dimensional SVEs and the results show that the three-dimensional SVEs consistently yield higher macroscale diffusivities by 17 % to 40 %, see Figure 5.4. The difference in numerical results is expected to depend on the fact that by truncating the third spatial dimension, a constraint is imposed on the the flux to only exist in a two-dimensional plane. In this way, the flux can only bypass an aggregate in the plane, but in 3D the out of plane solution is also possible, which yields higher diffusivity.

Additionally, the numerical results coincide with the upper Hashin-Shtrikman bound in the case of a two-phase mesoscale model of cement paste and aggregates. For three-phase concrete, the Taylor assumption yields a good estimate compared to computational homogenization of the macroscale diffusivity in the case of linear material properties on the mesoscale.

The numerical results further show that the ITZ implementation can be used to increase the obtained macroscale diffusivity by an arbitrary scale factor in an easy and efficiently way; thereby, enabling the model to be used for calibrating the diffusivity of

the ITZ with experimental data.

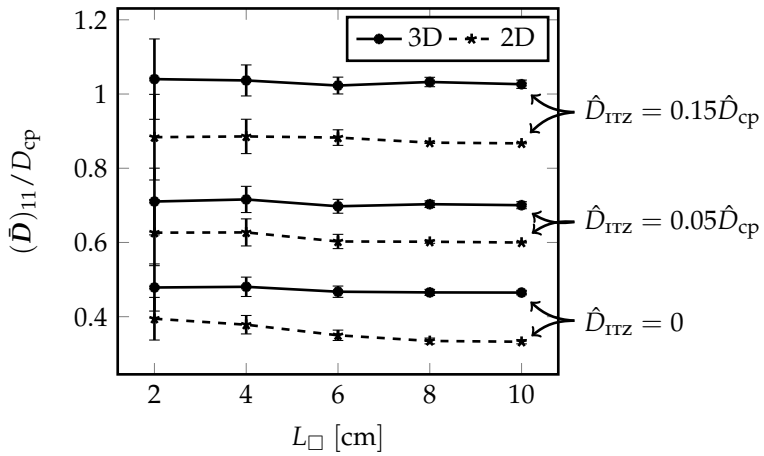

Figure 5.4: *Effective diffusivities as functions of SVE size and ITZ diffusivities. Error bars show mean values ± one standard deviation. The plots show that for any given ITZ diffusivity, $\hat{D}_{\text{ITZ}}$, the 2D SVEs consistently yield lower effective diffusivities, regardless of SVE size, $L_{\square}$.*

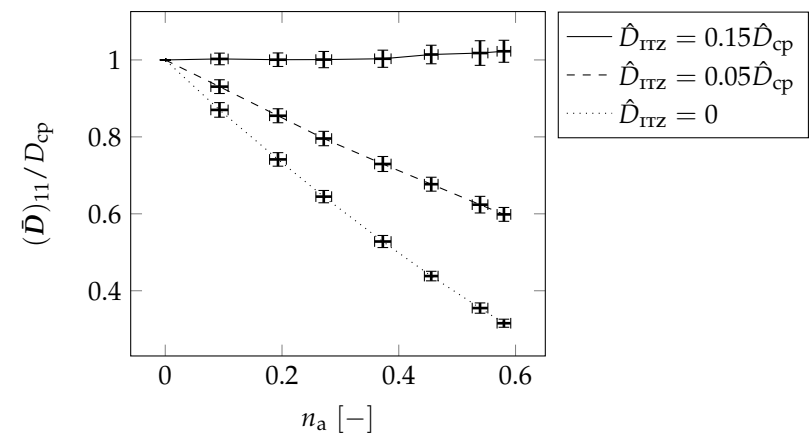

Figure 5.5: *Effective diffusivities as functions of volume aggregate contents, n_{a}, and different ITZ diffusivities. Theses results are similar to those obtained in **Paper A**, cf. Figure 5.1, even though a different sieve curves were used to generate RVEs and n_{a} represents area and volume aggregate content in 2D and 3D, respectively.*

Paper D: "Computational homogenization of crack-induced diffusivity in concrete"

The SVE model developed in **Paper C** was here further expanded to account for crack-induced diffusivity in concrete. Crack modelling was carried out using a smeared crack approach by means of an isotropic damage model for an SVE subjected to uniaxial tension loading. The ITZ was modelled to be transversal isotropic to capture the weak bond between the cement paste and aggregates. As a consequence, cracks were initiated in the ITZ and became interconnected in later stages of the simulation when a full crack was forming in the cement paste.

The cracked elements were assigned a diffusivity on the from given in Eq. (4.6.3) and the macroscopic diffusivity of concrete could as a result be established as a function of applied macroscale strain. The main computational results are shown in Figure 5.6.

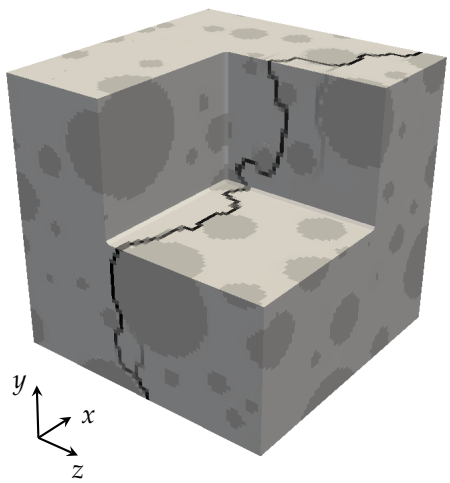

(a) *Cut out in an SVE showing how the crack path follows the weak interface between the cement paste and aggregates.*

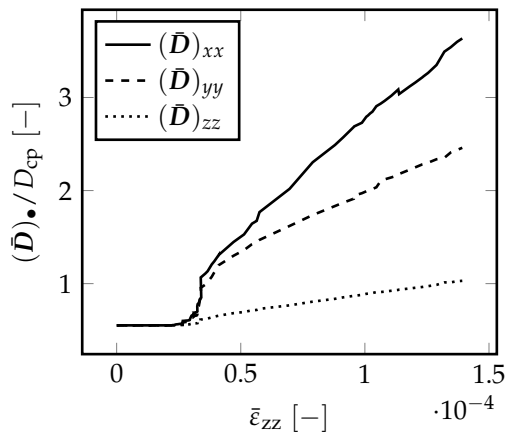

(b) *Diagonal components of the macroscale diffusivity tensor, $\bar{\boldsymbol{D}}$, as a function of macroscale strain. Numerical values are normalized with respect to D_{cp}. When the crack is initiated about $\bar{\varepsilon}_{zz} = 3 \times 10^{-5}$ the diffusivity increases rapidly in value.*

Figure 5.6: *Main computational results from **Paper D** where the influence of cracks on the macroscopic diffusivity is modelled. The SVE (left) is subjected to uni-axial tension loading and the macroscale diffusivity is determined as a function of applied macroscale strain (right). The anisotropy of the macroscale diffusivity due to cracks is captured by this model.*

6 Conclusions and outlook

The goal of this work was to model transport of moisture and chloride ions in concrete and to determine macroscale diffusivity by means of multiscale methods and computational homogenization. This goal was ultimately achieved by the development and implementation of two mesoscale models in two- and three dimensions.

The development of the mesoscale models shows that heterogeneities at the mesoscale level could be identified and distinguished as separate units of the material and could be accounted for by geometrical descriptions and separate constitutive relations. By this procedure, the material heterogeneities became parametrized and the influence on the macroscale behaviour of each individual mesoscale constituent—here in terms of cement paste, aggregates and the Interfacial Transition Zone (ITZ)—could therefore be studied in a straight-forward manner. This fact also implies that the material can be further parametrized by considering additional heterogeneities at e.g. finer length scales, such as the microscale.

The main conclusion from this work is that computational homogenization provides a rigorous theoretical framework and a useful numerical tool to model transport properties while accounting for mesoscale material heterogenities. A material can by this method be decomposed into its separate constituents, and concrete is naturally a very applicable material for this method due to its highly complex composition at the mesoscale. Additionally, in contrast to phenomenological models, the parameters pertaining to the mesoscale models are all physically sound quantities, e.g. volume fractions of aggregates and interface thickness of the ITZ. This is an appealing feature of this modelling approach if the model is to be used in conjunction with experimental work related to transport properties of concrete.

The numerical results obtained in this work show that the effects of the studied heterogeneities are ambiguous, but can be controlled in the model. For instance, the diffusivity of concrete is intuitively expected to decrease as the aggregate content increases since the aggregates can be assumed to be impermeable. However, an increase in aggregate content also means an increase in ITZ content and the ITZ has a higher diffusivity than the cement paste. Therefore, to estimate net effect of aggregates is computationally not a straight-forward task if all implications of aggregates are not fully considered and understood. Still, the net effect can by the developed model be controlled, and also calibrated with experimental data. This is an important outcome of the work, as it shows the potential of the model to yield realistic numerical simulations.

Additionally, this work forms a base where macroscale transport properties can be correlated to mechanical loading in a novel fashion. The numerical simulations carried out in this work showed how the macroscale diffusivity became anisotropic due to cracks forming in the SVE and that the macroscale diffusivity rapidly increased in magnitude once cracks had begun to develop. The crack propagation, in turn, could also be attributed to the material heterogenities of the SVE in a realistic way.

A suggestion for future work is the proper calibration with experimental data, which

has not been considered so far. This is crucial if one wants to carry out simulations with the aim of giving realistic predictions of moisture and chloride ingress in concrete. Such calibration could also determine which of the model parameters is of most importance and, hence, where more work needs to be allocated.

Furthermore, to extend the model down to the microscale would be an interesting path to take for future work. The cement paste is by no means a homogeneous material and to develop a corresponding heterogeneous microscale model in 3D would probably give further insights into the macroscopic behaviour of concrete.

References

[1] A. Ababneh, F. Benboudjema, and Y. Xi. "Chloride penetration in nonsaturated concrete". In: *Journal of Materials in Civil Engineering* 15.2 (2003), pp. 183–191. DOI: 10.1061/(ASCE)0899-1561(2003)15:2(183) (cit. on p. 5).

[2] A. Ababneh and Y. Xi. "An experimental study on the effect of chloride penetration on moisture diffusion in concrete". In: *Materials and Structures* 35.10 (Dec. 2002), pp. 659–663. ISSN: 1359-5997. DOI: 10.1007/BF02480359 (cit. on p. 5).

[3] D. Asahina and J. Bolander. "Voronoi-based discretizations for fracture analysis of particulate materials". In: *Powder Technology* 213.1-3 (Nov. 2011), pp. 92–99. ISSN: 00325910. DOI: 10.1016/j.powtec.2011.07.010 (cit. on p. 11).

[4] P. Austrell, O. Dahlblom, J. Lindemann, A. Olsson, K.-G. Olsson, K. Persson, H. Pettersson, M. Ristinmaa, G. Sandberg, and P.-A. Wernberg. *CALFEM: A Finite Element Toolbox : Version 3.4*. Structural Mechanics, LTH, 2004. ISBN: 91-8855823-1 (cit. on p. 2).

[5] V. Baroghel-Bouny, M. Thiéry, and X. Wang. "Modelling of isothermal coupled moisture–ion transport in cementitious materials". In: *Cement and Concrete Research* 41.8 (2011), pp. 828–841. ISSN: 00088846. DOI: 10.1016/j.cemconres.2011.04.001 (cit. on pp. 5, 7).

[6] K. J. Bathe. *Finite Element Procedures*. 1st. Prentice Hall, June 1995. ISBN: 0133014584 (cit. on p. 6).

[7] Z. P. Bažant and L. J. Najjar. "Nonlinear water diffusion in nonsaturated concrete". In: *Matériaux et Constructions* 5.1 (1972), pp. 3–20. DOI: 10.1007/BF02479073 (cit. on p. 5).

[8] D. P. Bentz, E. J. Garboczi, K. A. Snyder, N. I. of Standards, and T. (U.S.) *A hard core/soft shell microstructural model for studying percolation and transport in three-dimensional composite media*. U.S. Dept. of Commerce, Technology Administration, National Institute of Standards and Technology, 1999, 51 p. (Cit. on p. 11).

[9] R. B. Bird, W. E. Stewart, and E. N. Lightfoot. *Transport phenomena*. Revised second. John Wiley & Sons, 2007. ISBN: 978-0-470-11539-8 (cit. on p. 3).

[10] N. R. Buenfeld, M. Zobel, R. W. Zimmerman, and H. S. Wong. "Influence of the interfacial transition zone and microcracking on the diffusivity, permeability and sorptivity of cement-based materials after drying". In: *Magazine of Concrete Research* 61.8 (2009), pp. 571–589. ISSN: 0024-9831. DOI: 10.1680/macr.2008.61.8.571 (cit. on p. 14).

[11] A. Caballero, C. López, and I. Carol. "3D meso-structural analysis of concrete specimens under uniaxial tension". In: *Computer Methods in Applied Mechanics and Engineering* 195.52 (2006), pp. 7182–7195. ISSN: 00457825. DOI: 10.1016/j.cma.2005.05.052 (cit. on p. 11).

[12] I. Carol, A. Idiart, C. López, and A. Caballero. "Multiaxial behavior of concrete A mesomechanical approach". In: *European Journal of Environmental and Civil Engineering* 11.7-8 (2007), pp. 907–926. DOI: 10.3166/regc.11.907-926 (cit. on p. 11).

[13] R. Černý. "Experimental analysis of coupled water and chloride transport in cement mortar". In: *Cement and Concrete Composites* 26.6 (2004), pp. 705–715. ISSN: 09589465. DOI: 10.1016/S0958-9465(03)00102-1 (cit. on p. 5).

[14] R. Černý and P. Rovnaníková. *Transport processes in concrete*. London: Spon Press, 2002, p. 547. ISBN: 0415242649 (cit. on p. 3).

[15] L. De Lorenzis and P. Wriggers. "Computational homogenization of rubber friction on rough rigid surfaces". In: *Computational Materials Science* 77 (Sept. 2013), pp. 264–280. ISSN: 09270256. DOI: 10.1016/j.commatsci.2013.04.049 (cit. on p. 7).

[16] A. Delagrave, J. Bigas, J. P. Ollivier, J. Marchand, and M. Pigeon. "Influence of the interfacial zone on the chloride diffusivity of mortars". In: *Advanced Cement Based Materials* 5.3-4 (1997), pp. 86–92. ISSN: 10657355. DOI: 10.1016/S1065-7355(96)00008-9 (cit. on pp. 5, 16).

[17] S. Diamond and J. Huang. "The ITZ in concrete – a different view based on image analysis and SEM observations". In: *Cement and Concrete Composites* 23.2-3 (Apr. 2001), pp. 179–188. ISSN: 09589465. DOI: 10.1016/S0958-9465(00)00065-2 (cit. on p. 14).

[18] F. Feyel and J.-l. Chaboche. "FE^2 multiscale approach for modelling the elasto-viscoplastic behaviour of long fibre SiC/Ti composite materials". In: *Computer Methods in Applied Mechanics and Engineering* 183.3-4 (Mar. 2000), pp. 309–330. ISSN: 00457825. DOI: 10.1016/S0045-7825(99)00224-8 (cit. on p. 6).

[19] J. Fish, K. Shek, M. Pandheeradi, and M. S. Shephard. "Computational plasticity for composite structures based on mathematical homogenization: Theory and practice". In: *Computer Methods in Applied Mechanics and Engineering* 148.1-2 (Aug. 1997), pp. 53–73. ISSN: 00457825. DOI: 10.1016/S0045-7825(97)00030-3 (cit. on p. 6).

[20] E. Gal and R. Kryvoruk. "Meso-scale analysis of FRC using a two-step homogenization approach". In: *Computers and Structures* 89.11-12 (2011), pp. 921–929. ISSN: 0045-7949. DOI: 10.1016/j.compstruc.2011.02.006 (cit. on p. 7).

[21] E. J. Garboczi. "Multiscale Analytical/Numerical Theory of the Diffusivity of Concrete". In: *Advanced Cement Based Materials* 8.2 (1998), pp. 77–88. ISSN: 10657355. DOI: 10.1016/S1065-7355(98)00010-8 (cit. on pp. 7, 11).

[22] E. J. Garboczi and D. P. Bentz. "Modelling of the microstructure and transport properties of concrete". In: 10.5 (1996), pp. 293–300. ISSN: 09500618. DOI: 10.1016/0950-0618(94)00019-0 (cit. on p. 7).

[23] M. Geers, V. Kouznetsova, and W. Brekelmans. "Multi-scale computational homogenization: Trends and challenges". In: *Journal of Computational and Applied Mathematics* 234.7 (Aug. 2010), pp. 2175–2182. ISSN: 03770427. DOI: 10.1016/j.cam.2009.08.077 (cit. on p. 7).

[24] P. Grassl. "A lattice approach to model flow in cracked concrete". In: *Cement and Concrete Composites* 31.7 (2009), pp. 454–460. ISSN: 09589465. DOI: 10.1016/j.cemconcomp.2009.05.001 (cit. on p. 11).

[25] P. Grassl and T. Davies. "On a three-dimensional lattice approach for modelling corrosion induced cracking and its influence on bond between reinforcement and concrete". In: *Materials and Structures* (2010) (cit. on p. 11).

[26] P. Grassl and R. Rempling. "A damage-plasticity interface approach to the meso-scale modelling of concrete subjected to cyclic compressive loading". In: *Engineering Fracture Mechanics* 75.16 (2008), pp. 4804–4818. ISSN: 00137944. DOI: 10.1016/j.engfracmech.2008.06.005 (cit. on p. 11).

[27] M. Hain and P. Wriggers. "Computational homogenization of micro-structural damage due to frost in hardened cement paste". In: *Finite Elements in Analysis and Design* 44.5 (2008), pp. 233–244. ISSN: 0168874X. DOI: 10.1016/j.finel.2007.11.020 (cit. on pp. 7, 11).

[28] M. Hain and P. Wriggers. "Numerical homogenization of hardened cement paste". In: *Computational Mechanics* 42.2 (2007), pp. 197–212. ISSN: 0178-7675. DOI: 10.1007/s00466-007-0211-9 (cit. on pp. 7, 11).

[29] P. Halamickova, R. J. Detwiler, D. P. Bentz, and E. J. Garboczi. "Water permeability and chloride ion diffusion in portland cement mortars: Relationship to sand content and critical pore diameter". In: *Cement and Concrete Research* 25.4 (May 1995), pp. 790–802. ISSN: 00088846. DOI: 10.1016/0008-8846(95)00069-O (cit. on p. 5).

[30] A. E. Idiart, C. M. López, and I. Carol. "Chemo-mechanical analysis of concrete cracking and degradation due to external sulfate attack: A meso-scale model". In: *Cement and Concrete Composites* 33.3 (Mar. 2011), pp. 411–423. ISSN: 09589465. DOI: 10.1016/j.cemconcomp.2010.12.001 (cit. on p. 11).

[31] B. Johannesson. "A theoretical model describing diffusion of a mixture of different types of ions in pore solution of concrete coupled to moisture transport". In: *Cement and Concrete Research* 33.4 (Apr. 2003), pp. 481–488. ISSN: 00088846. DOI: 10.1016/S0008-8846(02)00993-6 (cit. on p. 5).

[32] B. Johannesson. "Nonlinear transient phenomena in porous media with special regard to concrete and durability". In: *Advanced Cement Based Materials* 6.3-4 (Oct. 1997), pp. 71–75. ISSN: 10657355. DOI: 10.1016/S1065-7355(97)90013-4 (cit. on p. 5).

[33] B. Johannesson. "Prestudy on diffusion and transient condensation of water vapor in cement mortar". In: *Cement and Concrete Research* 32.6 (June 2002), pp. 955–962. ISSN: 00088846. DOI: 10.1016/S0008-8846(02)00736-6 (cit. on p. 5).

[34] S. R. Kalidindi, M. Binci, D. Fullwood, and B. L. Adams. "Elastic properties closures using second-order homogenization theories Case studies in composites of two isotropic constituents". In: *Acta Materialia* 54 (2006), pp. 3117–3126. DOI: 10.1016/j.actamat.2006.03.005 (cit. on p. 7).

[35] T. Kanit, S. Forest, I. Galliet, V. Mounoury, and D. Jeulin. "Determination of the size of the representative volume element for random composites: statistical and numerical approach". In: *International Journal of Solids and Structures* 40.13-14 (June 2003), pp. 3647–3679. ISSN: 00207683. DOI: 10.1016/S0020-7683(03)00143-4 (cit. on p. 9).

[36] S. Kim and R. K. A. Al-rub. "Meso-scale computational modeling of the plastic-damage response of cementitious composites". In: *Cement and Concrete Research* 41.3 (2011), pp. 339–358. ISSN: 0008-8846. DOI: 10.1016/j.cemconres.2010.12.002 (cit. on p. 12).

[37] M. Koniorczyk and M. Wojciechowski. "Influence of salt on desorption isotherm and hygral state of cement mortar – Modelling using neural networks". In: 23.9 (2009), pp. 2988–2996. ISSN: 09500618. DOI: 10.1016/j.conbuildmat.2009.05.001 (cit. on p. 5).

[38] V. G. Kouznetsova, M. G. D. Geers, and W. A. M. Brekelmans. "Multi-scale second-order computational homogenization of multi-phase materials: a nested finite element solution strategy". In: *ComputerMethodsinAppliedMechanicsandEngineering* 193 (2004), pp. 5525–5550. DOI: 10.1016/j.cma.2003.12.073 (cit. on p. 6).

[39] F. Larsson, K. Runesson, and F. Su. "Variationally consistent computational homogenization of transient heat flow". In: *International Journal for Numerical Methods in Engineering* 81.13 (2009), pp. 1659–1686. ISSN: 00295981. DOI: 10.1002/nme.2747 (cit. on p. 6).

[40] L.-Y. Li, J. Xia, and S.-S. Lin. "A multi-phase model for predicting the effective diffusion coefficient of chlorides in concrete". In: *Construction and Building Materials* (2011). ISSN: 09500618. DOI: 10.1016/j.conbuildmat.2011.06.024 (cit. on p. 5).

[41] G. Lilliu and J. van Mier. "3D lattice type fracture model for concrete". In: *Engineering Fracture Mechanics* 70.7-8 (May 2003), pp. 927–941. ISSN: 00137944. DOI: 10.1016/S0013-7944(02)00158-3 (cit. on p. 11).

[42] A. Lindvall. "Environmental actions on concrete exposed in marine and road environments and its response Anders Lindvall". PhD thesis. 2003 (cit. on p. 5).

[43] MATLAB. *version 8.0.0.783 (R2012b)*. Natick, Massachusetts: The MathWorks Inc., 2012 (cit. on p. 2).

[44] P. K. Mehta and P. J. M. Monteiro. *Concrete: Microstructure, Properties and Materials*. McGraw-Hill Professional, 2006. ISBN: 0071462899. DOI: 10.1036/0071462899 (cit. on p. 3).

[45] C. Miehe, J. Schröder, and J. Schotte. "Computational homogenization analysis in finite plasticity Simulation of texture development in polycrystalline materials". In: *Computer Methods in Applied Mechanics and Engineering* 171.3-4 (Apr. 1999), pp. 387–418. ISSN: 00457825. DOI: 10.1016/S0045-7825(98)00218-7 (cit. on p. 6).

[46] S. Nemat-Nasser and M. Hori. *Micromechanics: Overall Properties of Heterogeneous Materials*. Elsevier, 1999. ISBN: 978-0-444-50084-7 (cit. on p. 6).

[47] T. T. Ngoc, J. Lewandowska, M. Vauclin, and H. Bertin. "Two-scale modeling of solute dispersion in unsaturated double-porosity media: Homogenization and experimental validation". In: *International Journal for Numerical and Analytical Methods in Geomechanics* 35.14 (Oct. 2011), pp. 1536–1559. ISSN: 03639061. DOI: 10.1002/nag.967 (cit. on p. 7).

[48] V. Nguyen, B. Nedjar, H. Colina, and J. Torrenti. "A separation of scales homogenization analysis for the modelling of calcium leaching in concrete". In: *Computer Methods in Applied Mechanics and Engineering* 195.52 (2006), pp. 7196–7210. ISSN: 00457825. DOI: 10.1016/j.cma.2005.02.036 (cit. on p. 7).

[49] A. U. Nilsen and P. J. Monteiro. "Concrete: A three phase material". In: *Cement and Concrete Research* 23.1 (Jan. 1993), pp. 147–151. DOI: 10.1016/0008-8846(93)90145-Y (cit. on p. 14).

[50] J. P. Ollivier, J. C. Maso, and B. Bourdette. "Interfacial transition zone in concrete". In: *Advanced Cement Based Materials* 2.1 (Jan. 1995), pp. 30–38. ISSN: 10657355. DOI: 10.1016/1065-7355(95)90037-3 (cit. on p. 14).

[51] M. Ostoja-Starzewski. "Material spatial randomness: From statistical to representative volume element". In: *Probabilistic Engineering Mechanics* 21.2 (Apr. 2006), pp. 112–132. ISSN: 02668920. DOI: 10.1016/j.probengmech.2005.07.007 (cit. on p. 9).

[52] I. Özdemir, W. Brekelmans, and M. Geers. "FE^2 computational homogenization for the thermo-mechanical analysis of heterogeneous solids". In: *Computer Methods in Applied Mechanics and Engineering* 198.3-4 (2008), pp. 602–613. ISSN: 00457825. DOI: 10.1016/j.cma.2008.09.008 (cit. on p. 6).

[53] S. Poyet. "Experimental investigation of the effect of temperature on the first desorption isotherm of concrete". In: *Cement and Concrete Research* 39.11 (2009), pp. 1052–1059. ISSN: 00088846. DOI: 10.1016/j.cemconres.2009.06.019 (cit. on p. 5).

[54] W. Puatatsananon and V. E. Saouma. "Nonlinear Coupling of Carbonation and Chloride Diffusion in Concrete". In: *Journal of Materials in Civil Engineering* 17.3 (2005), p. 264. DOI: 10.1061/(ASCE)0899-1561(2005)17:3(264) (cit. on p. 5).

[55] P. E. Roelfstra, H. Sadouki, and F. H. Wittmann. "Le béton numérique". In: *Materials and Structures* 18.5 (Sept. 1985), pp. 327–335. ISSN: 0025-5432. DOI: 10.1007/BF02472402 (cit. on p. 11).

[56] E. Schlangen and J. G. M. Mier. “Simple lattice model for numerical simulation of fracture of concrete materials and structures”. In: *Materials and Structures* 25.9 (Nov. 1992), pp. 534–542. ISSN: 0025-5432. DOI: 10.1007/BF02472449 (cit. on p. 11).

[57] N. Silva. “Chloride Induced Corrosion of Reinforcement Steel in Concrete – Threshold Values and Ion Distributions at the Concrete-Steel Interface”. PhD thesis. Chalmer University of Technology, 2013 (cit. on p. 5).

[58] T. Stankowski. “Numerical simulation of failure in particle composites”. In: *Computers & Structures* 44.1-2 (1992), pp. 459–468. ISSN: 00457949. DOI: 10.1016/0045-7949(92)90268-5 (cit. on p. 11).

[59] F. Su, F. Larsson, and K. Runesson. “Computational homogenization of coupled consolidation problems in micro-heterogeneous porous media”. In: *International Journal for Numerical Methods in Engineering* 88.11 (Dec. 2011), pp. 1198–1218. ISSN: 00295981. DOI: 10.1002/nme.3221 (cit. on p. 6).

[60] A. Suwito, X.-C. Cai, and Y. Xi. “Parallel Finite Element Method for Coupled Chloride and Moisture Diffusion in Concrete”. In: *International Journal for Numerical Analysis and Modeling* 3.4 (2006), pp. 481–503 (cit. on p. 5).

[61] L. Tang and L.-O. Nilsson. “Chloride Binding Capacity and Binding Isotherms of OPC Pastes and Mortars”. In: *Cement and Concrete Research* 23 (1993), pp. 247–253 (cit. on p. 5).

[62] L. Tang and L.-O. Nilsson. “A study of the quantitative relationship between permeability and pore size distribution of hardened cement pastes”. In: *Cement and Concrete Research* 22.4 (July 1992), pp. 541–550. ISSN: 00088846. DOI: 10.1016/0008-8846(92)90004-F (cit. on p. 5).

[63] K. Terada. “Simulation of the multi-scale convergence in computational homogenization approaches”. In: *International Journal of Solids and Structures* 37.16 (2000), pp. 2285–2311. DOI: 10.1016/S0020-7683(98)00341-2 (cit. on p. 7).

[64] G. Vanderheijden, R. Vanbijnen, L. Pel, and H. Huinink. “Moisture transport in heated concrete, as studied by NMR, and its consequences for fire spalling”. In: *Cement and Concrete Research* 37.6 (2007), pp. 894–901. ISSN: 00088846. DOI: 10.1016/j.cemconres.2007.03.004 (cit. on p. 5).

[65] L. Wang and T. Ueda. “Mesoscale modeling of water penetration into concrete by capillary absorption”. In: *Ocean Engineering* 38.4 (2011), pp. 519–528. ISSN: 00298018. DOI: 10.1016/j.oceaneng.2010.12.019 (cit. on pp. 11, 12).

[66] Y. Wang, L.-Y. Li, and C. Page. “Modelling of chloride ingress into concrete from a saline environment”. In: *Building and Environment* 40.12 (Dec. 2005), pp. 1573–1582. DOI: 10.1016/j.buildenv.2005.02.001 (cit. on p. 5).

[67] C. Wellmann, C. Lillie, and P. Wriggers. “Homogenization of granular material modeled by a three-dimensional discrete element method”. In: *Computers and Geotechnics* 35.3 (2008), pp. 394–405. ISSN: 0266352X. DOI: 10.1016/j.compgeo.2007.06.010 (cit. on p. 7).

[68] P. Wriggers and S. O. Moftah. “Mesoscale models for concrete : Homogenisation and damage behaviour”. In: *Finite Elements in Analysis and Design* 42 (2006), pp. 623–636. DOI: 10.1016/j.finel.2005.11.008 (cit. on p. 7).

[69] Y. Xi and Z. P. Bažant. “Modeling Chloride Penetration in Saturated Concrete”. In: *Journal of Materials in Civil Engineering* 11.1 (1999), pp. 58–66. ISSN: 08991561. DOI: 10.1061/(ASCE)0899-1561(1999)11:1(58) (cit. on pp. 5, 12).

[70] Y. Xi, Z. P. Bažant, L. Molina, and M. Jennings. “Moisture diffusion in cementitious materials: Moisture capacity and diffusivity”. In: *Advanced Cement Based Materials* 1.6 (1994), pp. 258–266. ISSN: 10657355. DOI: 10.1016/1065-7355(94)90034-5 (cit. on pp. 5, 12).

[71] C. Yang and S. Cho. “Approximate migration coefficient of percolated interfacial transition zone by using the accelerated chloride migration test”. In: *Cement and Concrete Research* 35.2 (2005), pp. 344–350. ISSN: 00088846. DOI: 10.1016/j.cemconres.2004.05.038 (cit. on p. 14).

[72] C. Yang and S. Cho. “Influence of aggregate content on the migration coefficient of concrete materials using electrochemical method”. In: *Materials Chemistry and Physics* 80.3 (June 2003), pp. 752–757. ISSN: 02540584. DOI: 10.1016/S0254-0584(03)00112-3 (cit. on p. 14).

[73] K. Zandi Hanjari. “Structural Behaviour of Deteriorated Concrete Structures”. PhD thesis. Chalmer University of Technology, 2010 (cit. on p. 5).

[74] O. C. Zienkiewicz and R. L. Taylor. *Finite Element Method: Volume 1, Fifth Edition*. 5th ed. Butterworth-Heinemann, Sept. 2000. ISBN: 0750650494 (cit. on p. 6).